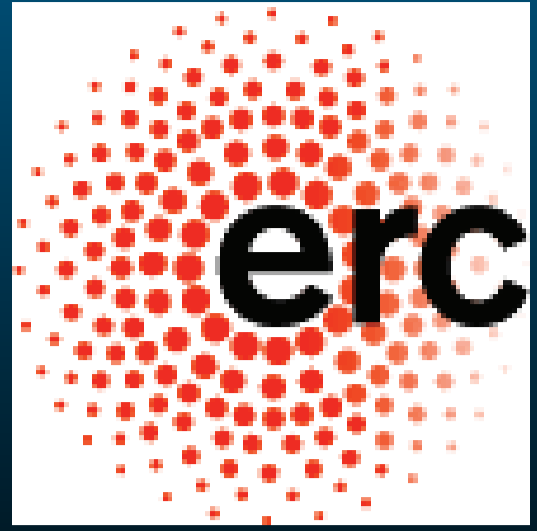


# Anisotropy effects in the Kondo insulator

## CeRu<sub>4</sub>Sn<sub>6</sub>

J. Hänel, H. Winkler, K.-A. Lorenzer, J. Custers, A. Prokofiev, A. Sidorenko and S. Paschen

Institute of Solid State Physics, Vienna University of Technology, 1040 Vienna, Austria



### Abstract

Kondo insulators represent a special class of heavy fermion systems where a half-filled conduction band hybridizes with an almost dispersionless 4f level resulting in a heavy quasiparticle band with a small energy gap of a few meV at the Fermi level. The tetragonal crystal structure of the Kondo insulator CeRu<sub>4</sub>Sn<sub>6</sub> (Figure 1) places it in between the archetypal cubic Kondo insulators like YbB<sub>12</sub> or Ce<sub>3</sub>Bi<sub>4</sub>Pt<sub>3</sub> and the orthorhombic Kondo semimetals CeNiSn and CeRhSb [1, 2]. Investigations of possible anisotropies - or even nodes - of the Kondo insulating gap in CeRu<sub>4</sub>Sn<sub>6</sub> are of central interest.

We show for the first time electrical resistivity, Hall effect and Hall mobility data of single crystals of this compound along three different crystallographic directions. Magnetic susceptibility and magnetization data shown previously [3] are complemented with data obtained from torque measurements. Large anisotropy effects are revealed in all these physical properties, both between the tetragonal *c* direction and the basal plane and within a quasi cubic cell arising in this compound due to the lattice parameter in the [0 0 1] direction almost matching the lattice spacing in the [1 1 0] direction [3].

### Results

Figure 5 shows the temperature dependence of the electrical resistivity. It resembles the behaviour typically found in Kondo insulators.

Dc susceptibility measured with a SQUID magnetometer along the crystallographic directions [1 0 0], [0 0 1] and [1 1 0] is displayed in Figures 2 and 3. The *c*-axis is identified as the hard axis. The value of the susceptibility in this direction,  $\chi_c$ , was remeasured by means of torque magnetometry. The torque data reveal a significantly lower value of  $\chi_c$  than measured directly in a SQUID. The same effect is observed in the magnetization data (Figure 4). This is attributed to the torque magnetometry being less prone to misalignments of the sample.

Figures 6 and 7 show the Hall constant and the Hall mobility with the current applied along the three different crystallographic directions. The field is always applied perpendicular to the current. The mobility data again shows pronounced anisotropy between the *a*- and *c*-, as well as between the *c'*- and *c*-direction.

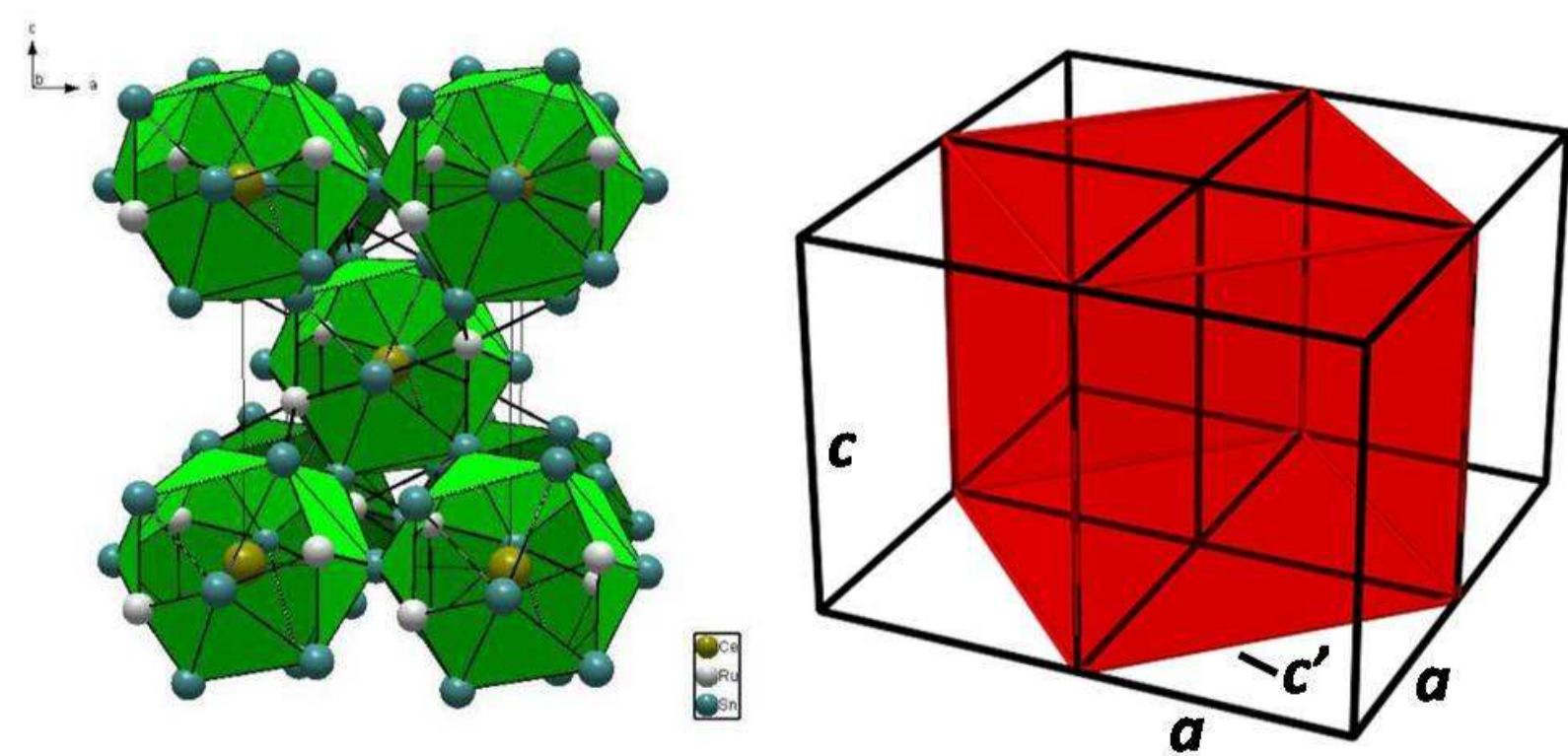


FIGURE 1: Crystal structure of CeRu<sub>4</sub>Sn<sub>6</sub> and scheme of the quasi cubic cell within the tetragonal cell.

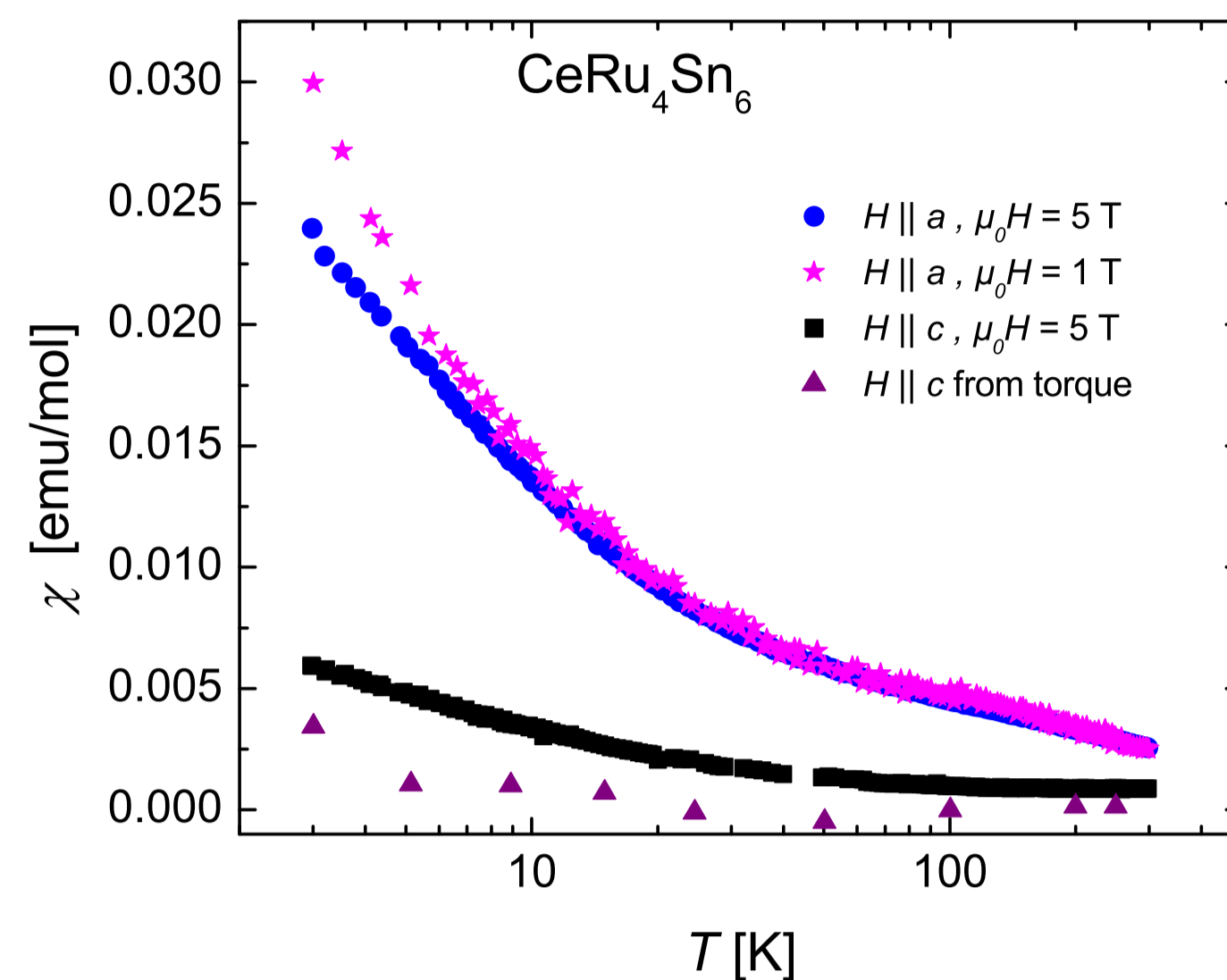


FIGURE 2: Temperature dependence of the magnetic susceptibility,  $\chi(T)$ , of a CeRu<sub>4</sub>Sn<sub>6</sub> single crystal with field applied along the *a*- and the *c*-direction. Comparison of the SQUID data with susceptibility  $\chi_c(T)$  computed from torque data.

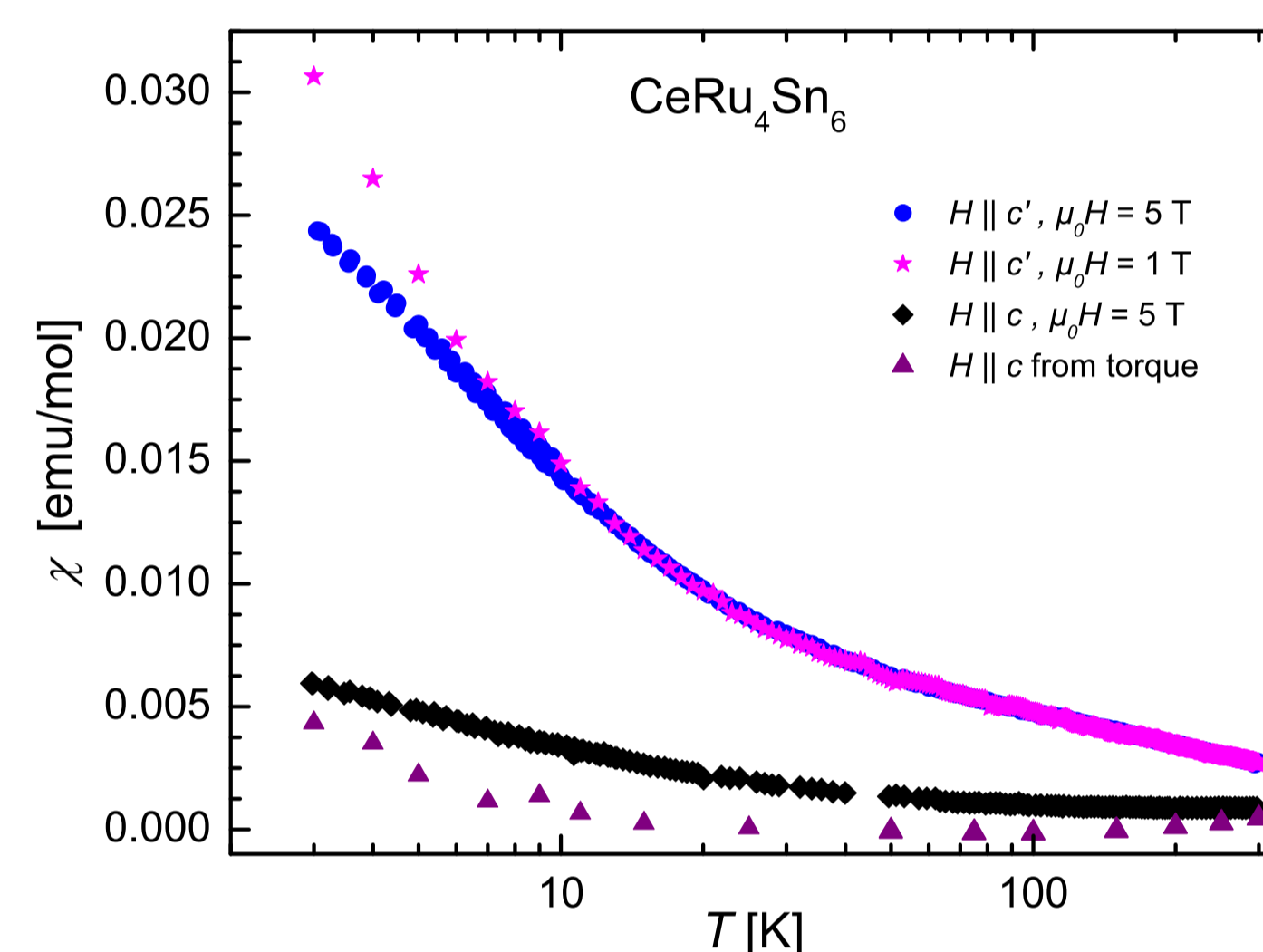


FIGURE 3: Temperature dependence of the magnetic susceptibility,  $\chi(T)$ , of a CeRu<sub>4</sub>Sn<sub>6</sub> single crystal with field applied along the *c'*- and the *c*-direction. Comparison of the SQUID data with susceptibility  $\chi_c(T)$  computed from torque data.

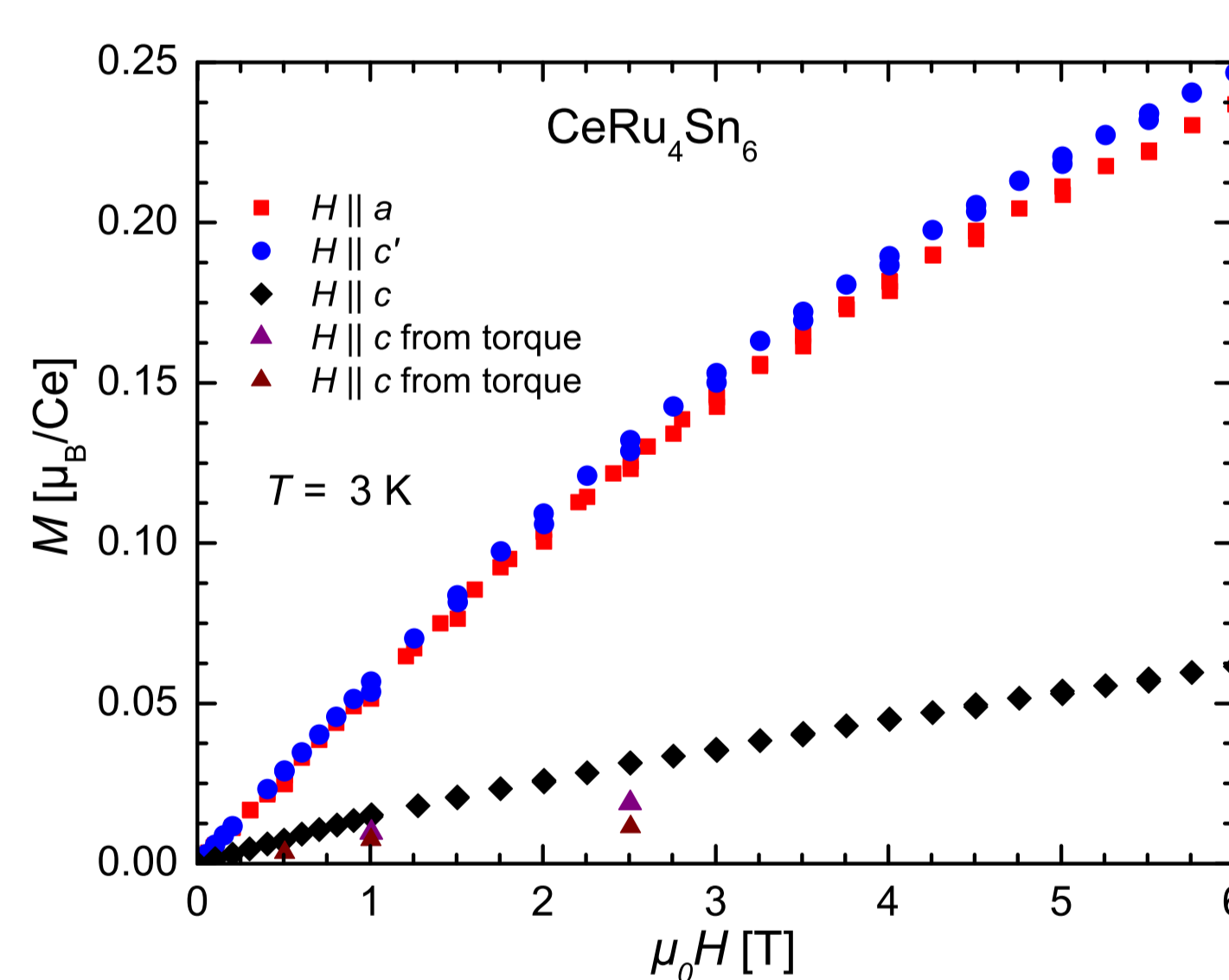


FIGURE 4: Magnetic field dependence of the magnetization,  $M(\mu_0 H)$ , of CeRu<sub>4</sub>Sn<sub>6</sub>, taken at 3 K for fields applied along the three crystallographic directions *a*, *c* and *c'*. Comparison of the SQUID data with magnetization  $M_c(\mu_0 H)$  computed from torque data.

### Interpretation

A crystal field model can describe  $\chi_a$  and  $\chi_{c'}$ , but fails to account for the very small values of  $\chi_c$ . We attribute this to the opening of an energy gap along *c*.

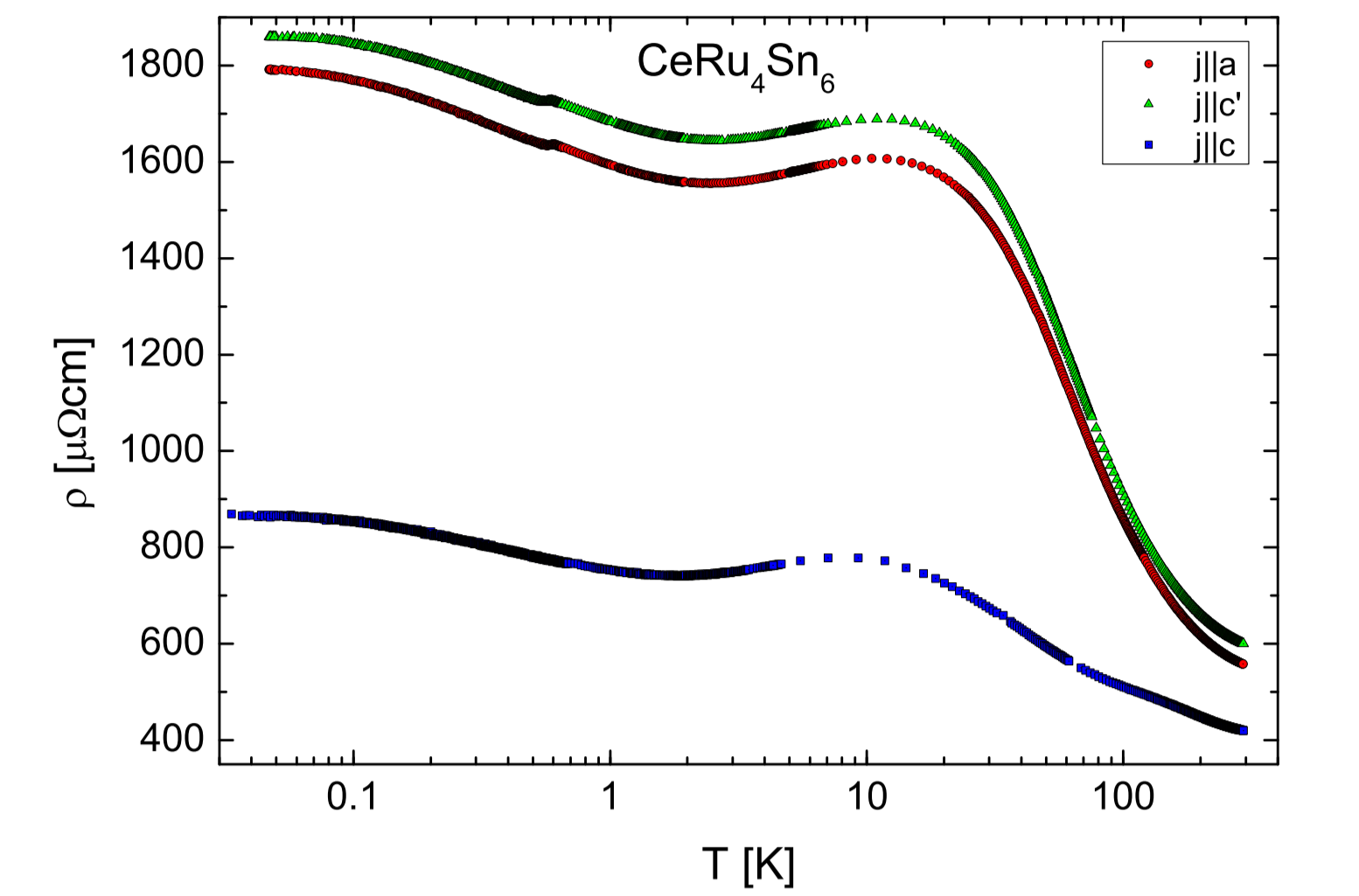


FIGURE 5: Temperature dependence of the electrical resistivity,  $\rho(T)$ , of single crystalline CeRu<sub>4</sub>Sn<sub>6</sub> with the current applied along the crystallographic directions *a*, *c* and *c'*.

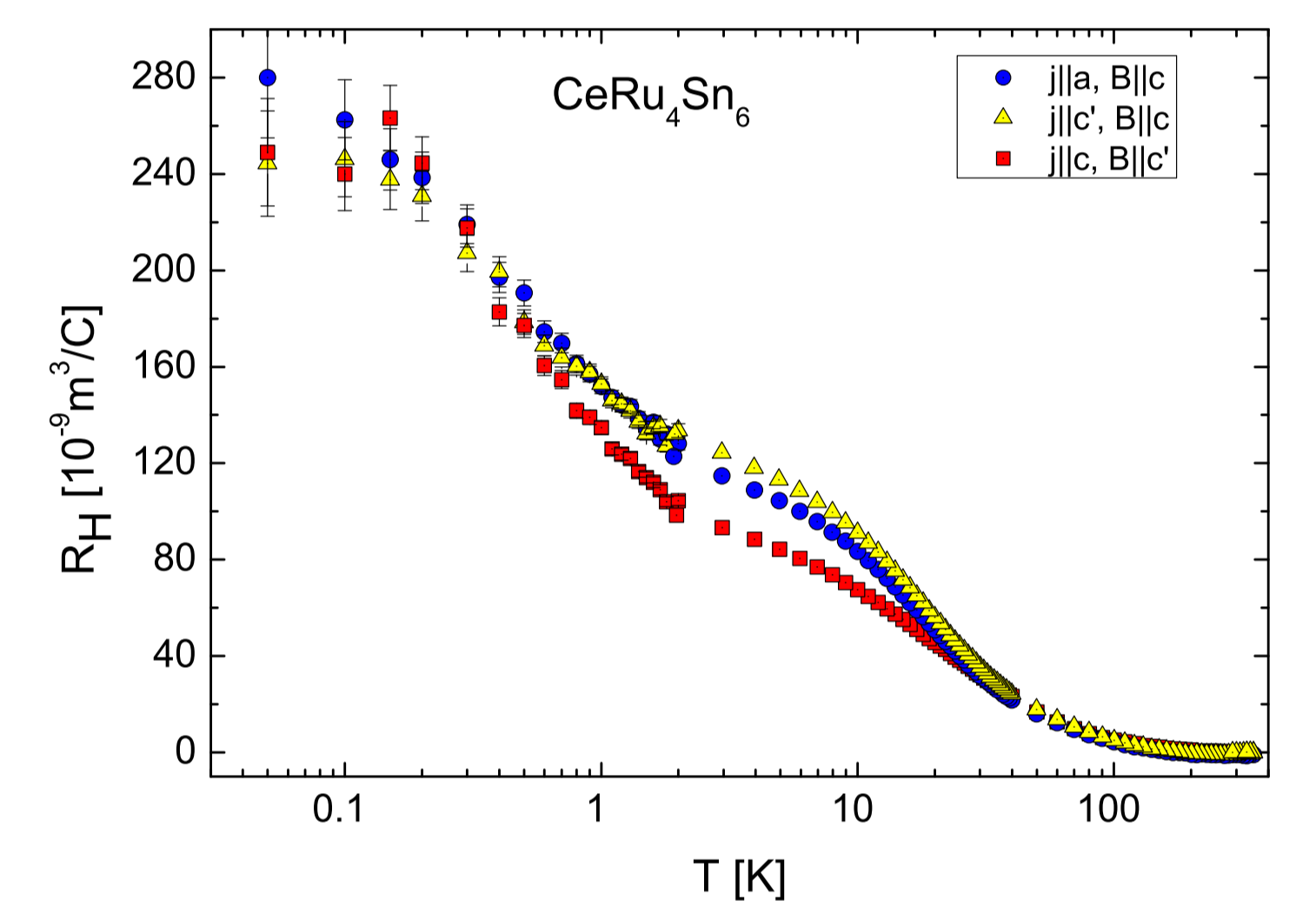


FIGURE 6: Temperature dependence of the Hall constant  $R_H(T)$  of a CeRu<sub>4</sub>Sn<sub>6</sub> single crystal, with the current along *a*, *c* and *c'*.

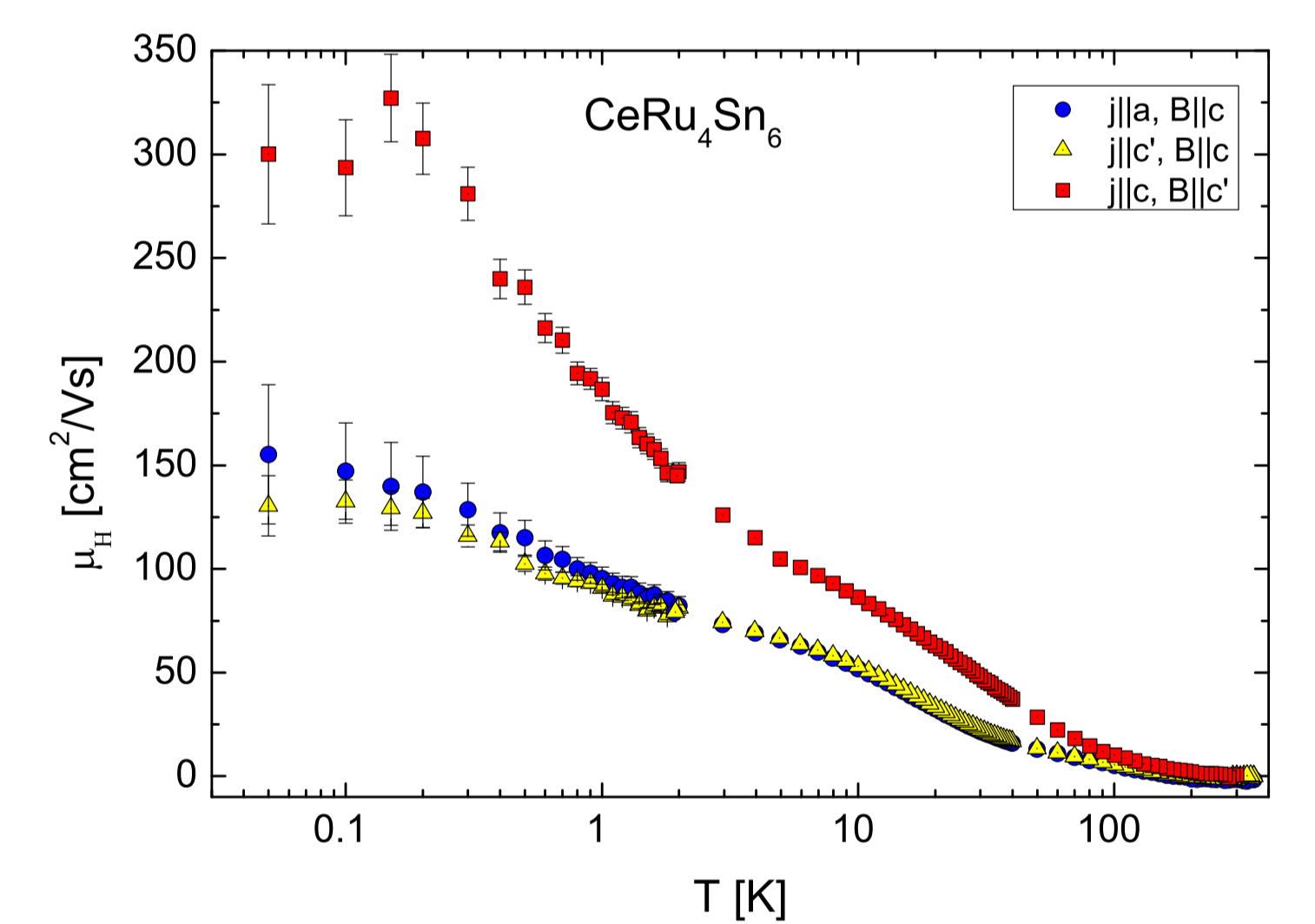


FIGURE 7: Temperature dependence of the Hall mobility,  $\mu_H(T)$ , of a CeRu<sub>4</sub>Sn<sub>6</sub> single crystal, with the current along *a*, *c* and *c'*.

### Conclusion

Anisotropy is observed in all the examined physical properties along the fundamental crystal directions of CeRu<sub>4</sub>Sn<sub>6</sub>.

### Acknowledgements

This work was supported by the ERC Advanced Researcher Grant No. 227378.

### References

- [1] G. Aeppli and Z. Fisk, *Comments Condens. Matter Phys.* **16**, (1992) 155.
- [2] A.M. Strydom, Z. Guo, S. Paschen, R. Viennois, F. Steglich, *Physica B* **359-361** (2005) 293.
- [3] S. Paschen, H. Winkler, T. Nezu, M. Kriegisch, G. Hilscher, J. Custers, A. Prokofiev, *J. Phys.: Conf. Ser.* **012156** (2010) 200.



TECHNISCHE  
UNIVERSITÄT  
WIEN  
Vienna University of Technology

Contact for this poster: J. Hänel  
jonathan.haenel@tuwien.ac.at  
Phone: +43 1 58801 13183